

High NA Absolute Fizeau Phase Shifting Interferometry

Joachim Wesner, Joachim Heil and Hans-Martin Heuck

Leica Microsystems CMS GmbH, Ernst-Leitz-Strasse 17-37, D-35578 Wetzlar, Germany

<mailto:joachim.wesner@leica-microsystems.com>

The aperture range of axial Fizeau PSI usually limited by shift non-uniformity can be extended to $NA \approx 0.95$ using advanced PSI algorithms and proper shift tuning. Here, the exact form of the defocusing term needs to be taken into account to avoid apparent spherical aberrations upon inevitable axial maladjustment. These extensions combined with an "N+1 position" absolute test promise for accuracies $< \lambda/100$ using commercial systems, as illustrated on hemispherical concave mirrors compared to results obtained with a custom Twyman-Green (TG) setup.

1 High NA axial translation Fizeau PSI

PSI in a Fizeau interferometer by axial translation of the transmission sphere TS causes phase shifts $\sim \cos(\theta)$, introducing phase reconstruction errors. This restricts its application to $f\# < 0.75$ ($NA > 0.67$), which can be overcome by employing advanced algorithms. Their full error tolerance is exploited by redistributing the shift error over the pupil [1]. For a typical "High-Res" 13-step algorithm, increasing the "piezo gain" by a factor ≈ 1.5 will assure a phase error $< \lambda/100$ up to $NA \approx 0.95$ (Fig. 1, 2).

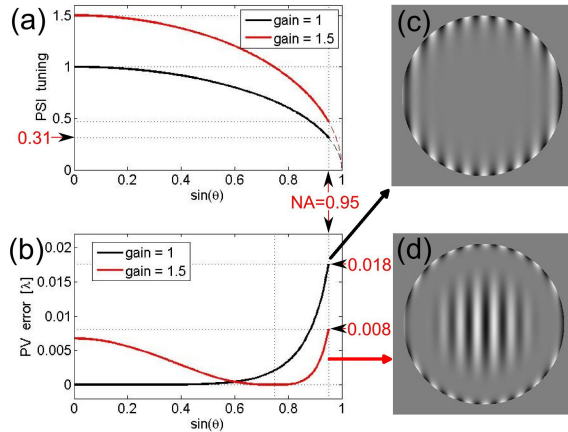


Fig. 1 Phase shift tuning (a) and predicted phase error (b) for the 13-step PSI algorithm including symmetrization (red). Simulated phase reconstruction errors (c,d)

2 High NA defocus and spherical aberration

At high NA, Zernike "piston" $z_{0,0}$ and parabolic "power" $z_{2,0}$ yield only a poor approximation of a spherical wave front axially displaced by d (Fig. 2)

$$\begin{aligned} OPD(\theta)/d &= \cos \theta \approx 1 - \theta^2/2 \approx 1 - r^2 NA^2/2 = \dots \\ (1 - NA^2/4) - NA^2/4 \cdot (2r^2 - 1) &= z_{0,0} + z_{2,0} \cdot Z_{2,0}(r) \end{aligned} \quad (1)$$

If only $z_{0,0}$ and $z_{2,0}$ are removed (as usual), ignoring higher terms introduces varying apparent spherical aberration when residual defocus is present. At $NA=0.95$, $d=1\lambda$ causes an error of $\approx \lambda/20$ in $z_{4,0}$, Fig. 3 (b). Note that proper focusing is quite tricky

at high NA, also because typical instruments idle at the end of the shift range up to 1λ displaced from mid-shift, being relevant for phase reconstruction.

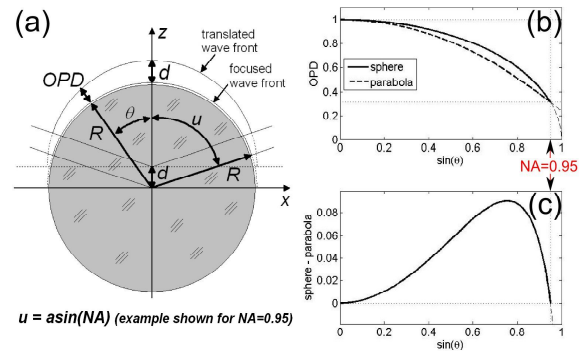


Fig. 2 High NA defocusing (a), spherical OPD and related paraboloid (b), apparent spherical aberration (c)

For a TS satisfying the sine condition, the proper Zernike decomposition of a defocusing OPD is:

$$z_{2n,0}^{spher}(d) = d \cdot \int_0^1 \sqrt{1 - r^2 NA^2} Z_{2n,0}(r) r dr. \quad (2)$$

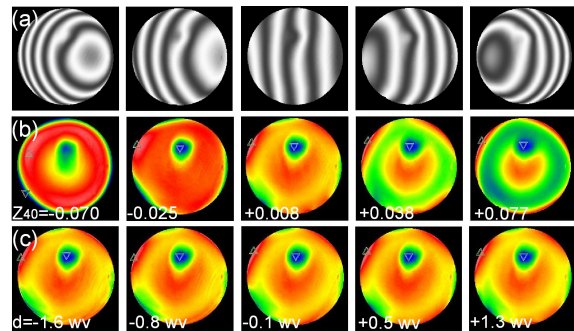


Fig. 3 Reconstructing a test surface S for different defocus d at $NA=0.94$: (a) fringe pattern at shift center, (b) Reconstruction using "power removal", and (c) "sphere removal" based on Eq. (2)

Validity of (2) for a $NA=0.94$ TS was checked from the measured $z_{2n,0}$ versus defocus (Fig. 4), the slopes agreeing well with the theory (0.154, 0.044, 0.015), the small difference for $z_{8,0}$ being irrelevant.

Correct removal of high NA defocus was realized using (2) by subtracting a spherical wave of given NA with the measured amount of $z_{2,0}$. This result is shown in Fig. 3, (c), now consistently revealing the inherent aberrations of test surface S (with an intentionally introduced pit), however, with the error of the reference surface R still superimposed.

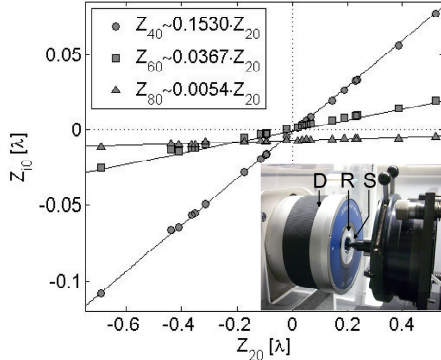


Fig. 4 Measured spherical aberrations Z_{40} , Z_{60} , Z_{80} versus defocus (expressed as z_{20}) for a $f\#=0.53$ ($NA=0.94$) TS. Inset illustrates setup and contributions S , R and D

3 N+1 position absolute test

The “ N -fold” azimuthal average NF (with the properties of a projection operator [2]) of a wave field W and its “non- N -fold” complement NF_C are

$$NF(W) = 1/N \sum_{i=0}^{N-1} Rot(W, 2\pi i/N), \quad (3)$$

$$NF_C(W) = W - NF(W),$$

here, $Rot(W, \varphi)$ rotates W by φ .

Note that $2F$ is equivalent to the “even” and $2F_C$ to the “odd” part of W , while NF and NF_C turn into the rotationally symmetric (RS) and non-symmetric (NRS) parts for $N \rightarrow \infty$. Also, NF completely removes all azimuthal (e.g. Zernike) terms of angular frequency not an integer multiple $m \geq 0$ of N [3].

In the “ $N+1$ position absolute test”, three quantities A , B and C are determined. A is acquired by rotating the sample surface S with respect to the reference sphere R into N azimuth positions and averaging the resulting wave fronts W_i . The same W_i are de-rotated numerically and averaged to yield B . Cat’s-eye data W_{CE} are NF -filtered, removing the effect of the diverger D if N is even, giving C .

$$A = 1/N \sum W_i = NF(S) + R, \quad (4)$$

$$B = 1/N \sum Rot(W_i, -2\pi i/N) = S + NF(R), \quad (5)$$

$$C = NF(W_{CE}) = NF(R + Odd(D)) = NF(R). \quad (6)$$

S and R are then most easily found as:

$$S = B - C, \quad \text{and} \quad R = NF_C(A) + C. \quad (7)$$

This procedure, while valid for any N , can best be understood for $N \rightarrow \infty$, where C is the RS part of R which is subtracted from B to give S . For R , the erroneous RS part of A can be directly replaced by C using symmetry only. For $N=2$, (4-7) reduce to the well-known “2-sphere” test, averaging W_{0° and W_{180° to calculate R , instead of the less accurate (as to noise) but common treatment of only using W_{0° . Our procedure is also equivalent to averaging multiple “2-sphere” tests for $N > 2$. For increasing N , most of the angular information of R and S is retrieved from W_i , while the relevant information in W_{CE} are the RS terms only, e.g. $N=6$ being sufficient for 36 Zernikes, $N=12$ for 144 Zernikes [3].

4 Experimental high NA absolute Fizeau results

The techniques in chapters 1-3 were combined to measure several high NA surfaces (Fig. 5):

For the sphere with the artificial pit (Fig. 3), R was independently determined using so-called “ball averaging” in (b), yielding S in (c). This compares favorably to the 8 azimuth position results in (d) where artifacts from R are completely removed.

Several hemispherical mirrors were also tested at 8 azimuths with the $NA=0.94$ TS in (e-h) and verified in a TG-setup in (i-l) using a $NA=0.90$ micro-objective (in the TG case, Eqs. (4-7) were solved using a 121 (20th order) Zernike fit, instead of raw data), (b) and (c) compare nicely at the $\lambda/100$ level.

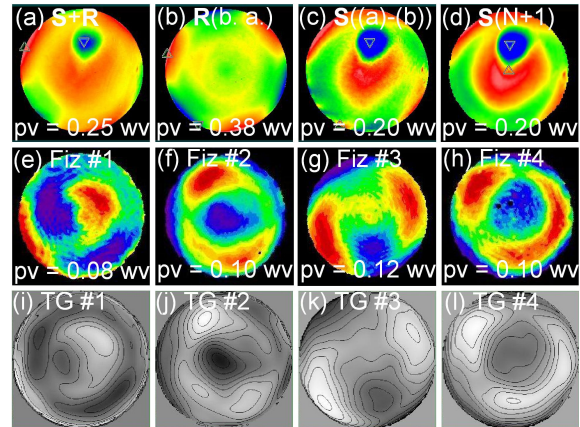


Fig. 5 (a) $S+R$ from Fig. 3, (b) R from “ball averaging”, (c) S from (a)-(b), (d) S from a “8+1 test”. (e-h) hemispherical concave mirrors measured with a $NA=0.94$ Fizeau TS with the “8+1 test”, (i-l) corresponding data taken in a TG-setup at $NA=0.9$. Isolines spacing = $\lambda/100!$

References

- [1] P. de Groot: “Phase-shift calibration errors in interferometers with spherical Fizeau cavities”, *Appl. Opt.* **34**, 2856-63 (1995)
- [2] U. Griesmann, “Three-flat test solutions based on simple mirror symmetry”, *Appl. Opt.* **45**, 5856-65 (2006)
- [3] C. J. Evans, R. N. Kestner: “Test optics error removal”, *Appl. Opt.* **35**, 1015-21 (1996)